Measurement of the proton electric to magnetic form factor ratio from $^1\vec{\text{H}}(\vec{e}, e'\text{p})$

C.B. Crawford,[1] A. Sindile,[2] T. Akdogan,[1] R. Alarcon,[3] W. Bertozzi,[1] E. Booth,[4] T. Botto,[1] J. Calarco,[2]

B. Clasie,[1] A. DeGrush,[1] T.W. Donnelly,[1] K. Dow,[1] D. Dutta,[5] M. Farkhondeh,[1] R. Fatemi,[1] O. Filoti,[2]

W. Franklin,[1] H. Gao,[5] E. Geis,[3] S. Gilad,[1] W. Haeberli,[6] D. Hasell,[1] W. Hersman,[2] M. Holtrop,[2]

P. Karpius,[2] M. Kohl,[1] H. Kolster,[1] T. Lee,[2] A. Maschinot,[1] J. Matthews,[1] K. McIlhany,[7] N. Meitanis,[1]

R.G. Milner,[1] J. Rapaport,[8] R.P. Redwine,[1] J. Seely,[1] A. Shinozaki,[1] S. Širca,[1] E. Six,[3] T. Smith,[9]

B. Tonguc,[3] C. Tschalaer,[1] E. Tsentalovich,[1] W. Turchinetz,[1] J.F.J. van den Brand,[10] J. van der Laan,[1]

F. Wang,[1] T. Wise,[6] Y. Xiao,[1] W. Xu,[5] C. Zhang,[1] Z. Zhou,[1] V. Ziskin,[1] and T. Zwart[1]

[1]*Laboratory for Nuclear Science and Bates Linear Accelerator Center,*
Massachusetts Institute of Technology, Cambridge, MA 02139
[2]*University of New Hampshire, Durham, NH 03824*
[3]*Arizona State University, Tempe, AZ 85287*
[4]*Boston University, Boston, MA 02215*
[5]*Duke University, Durham, NC 27708-0305*
[6]*University of Wisconsin, Madison, WI 53706*
[7]*United States Naval Academy, Annapolis, MD 21402*
[8]*Ohio University, Athens, OH 45701*
[9]*Dartmouth College, Hanover, NH 03755*
[10]*Vrije Universitaet and NIKHEF, Amsterdam, The Netherlands*
(Dated: February 7, 2008)

We report the first precision measurement of the proton electric to magnetic form factor ratio from spin-dependent elastic scattering of longitudinally polarized electrons from a polarized hydrogen internal gas target. The measurement was performed at the MIT-Bates South Hall Ring over a range of four-momentum transfer squared Q^2 from 0.15 to 0.65 (GeV/c)^2. Significantly improved results on the proton electric and magnetic form factors are obtained in combination with previous cross-section data on elastic electron-proton scattering in the same Q^2 region.

The electromagnetic form factors of the nucleon are fundamental quantities describing the distribution of charge and magnetization within the nucleon. At low four-momentum transfer squared Q^2, they are sensitive to the pion cloud [1, 2], and provide tests of effective field theories of quantum chromodynamics (QCD) based on chiral symmetry [3]. Lattice QCD has made considerable progress in describing the form factors at low Q^2 [4] and, with future advances in technique and computing power, tests against precise data will be possible. Accurate measurements of nucleon electromagnetic form factors at low Q^2 are also important for interpretation of parity-violation electron scattering experiments [5], which probe the strange quark contribution to the nucleon electromagnetic structure. Knowledge of the internal structure of protons and neutrons in terms of the quark and gluon degrees of freedom of QCD provides a basis for understanding more complex, strongly interacting matter at the level of quarks and gluons.

The proton electric (G_E^p) and magnetic (G_M^p) form factors have been studied extensively in the past [6] over a wide range of Q^2 from unpolarized electron-proton (e-p) elastic scattering using the Rosenbluth (L-T) separation technique [7]. While the precise knowledge of the separated form factors G_E^p and G_M^p is important for understanding the underlying electromagnetic structure of the nucleon, it is also very interesting to study the ratio $\mu_p G_E^p / G_M^p$ as a function of Q^2, where $\mu_p \sim 2.79$ is the proton magnetic moment in units of nuclear magnetons. The observation of a Q^2 dependence in the form factor ratio would suggest different charge and current spatial distributions inside the proton.

Recent advances in polarized beams, targets, and polarimetry have made possible a new class of experiments extracting $\mu_p G_E^p / G_M^p$ utilizing spin degrees of freedom. Extraction of the form factor ratio from double polarization observables has two substantial advantages over unpolarized cross section measurements. First, the spin-dependent cross section has an interference term between G_E^p and G_M^p, allowing for a direct determination of $\mu_p G_E^p / G_M^p$ from either the spin-dependent asymmetry [8] or the recoil polarization measurement [9], whereas the unpolarized cross section depends only on the squares of G_E^p and G_M^p. Second, spin degrees of freedom can be varied instead of the beam energy and scattering angle (as is done in the Rosenbluth separation), greatly reducing the systematic errors. New data from polarization transfer experiments [10, 11] show a very intriguing behavior at higher Q^2: starting at $Q^2 = 1$ (GeV/c)^2, $\mu_p G_E^p / G_M^p$ drops linearly from approximately 1 down to 0.28 at the highest measured Q^2 value (~ 5.54 (GeV/c)^2). This is very different from unity, as suggested by previous unpo-

larized cross section measurements [12, 13] and verified by recent experiments [14, 15].

While the interesting Q^2 dependence of the proton form factor ratio from recoil polarization experiments [10, 11] has been described in terms of nonzero parton orbital angular momentum or hadron helicity flip [16, 17, 18, 19], it is important to understand the discrepancy between results obtained from recoil proton polarization measurements and those from the Rosenbluth method. Two-photon exchange contributions may contribute [20, 21] up to about half of the observed discrepancy between the two experimental methods, identifying the need for further experimental tests.

In this letter we report the first measurement of $\mu_p G_E^p / G_M^p$ from ${}^1\vec{\mathrm{H}}(\vec{\mathrm{e}}, \mathrm{e'p})$ in the Q^2 region between 0.15 and 0.65 $(\mathrm{GeV}/c)^2$ [22, 23], overlapping with the lower Q^2 region of the recoil polarization data [10, 24, 25, 26, 27]. This is an important region which allows for tests of effective field theory predictions and verifications of future precision results of Lattice QCD. It also helps to quantify the role of the pion cloud in the structure of the nucleon. The polarized target technique has different sources of systematic uncertainty than recoil polarimetry, but still benefits from the same cancellations in systematic uncertainties such as detection efficiency and luminosity.

In the one-photon exchange approximation, the elastic scattering asymmetry of longitudinally polarized electrons from polarized protons with respect to the electron beam helicity has the form [8]

$$A_{phys} = \frac{v_z \cos\theta^* G_M^{p\,2} + v_x \sin\theta^* \cos\phi^* G_M^p G_E^p}{(\tau G_M^{p\,2} + \epsilon G_E^{p\,2}) / [\epsilon(1+\tau)]}, \quad (1)$$

where θ^* and ϕ^* are the polar and azimuthal angles of the target polarization defined relative to the three-momentum transfer vector of the virtual photon and $\tau = Q^2/(4M_p^2)$ with the proton mass M_p. The longitudinal polarization of the virtual photon is denoted as $\epsilon = [1 + 2(1+\tau)\tan^2(\theta_e/2)]^{-1}$ where θ_e is the electron scattering angle, and $v_z = -2\tau \tan(\theta_e/2)\sqrt{1/(1+\tau) + \tan^2(\theta_e/2)}$, $v_x = -2\tan(\theta_e/2)\sqrt{\tau/(1+\tau)}$ are kinematic factors. The experimental asymmetry

$$A_{exp} = P_b P_t\, A_{phys} \quad (2)$$

is reduced by the beam (P_b) and target (P_t) polarizations.

The form factor ratio $\mu_p G_E^p / G_M^p$ and the polarization product $P_b P_t$ can be determined by measuring two experimental asymmetries A_l and A_r at the same Q^2 value, but with different spin orientations (θ_l^*, ϕ_l^*) and (θ_r^*, ϕ_r^*), respectively. For a detector configuration that is symmetric about the incident electron beam and with the target polarization angle oriented $\sim 45°$ to the left of the beam, A_l and A_r can be measured simultaneously by forming two independent asymmetries of electrons scattered into the beam-left and beam-right sectors, respectively. In this case A_l (A_r) is predominantly transverse (longitudinal).

The Bates Large Acceptance Spectrometer Toroid (BLAST) experiment was carried out in the South Hall Ring of the MIT Bates Linear Accelerator Center, which stored an intense polarized beam with a beam current of up to 225 mA and longitudinal electron polarization of 65%. A 180° spin rotator (Siberian Snake) was used in the ring opposite the interaction point to preserve the longitudinal electron polarization at the target, which was continuously monitored with a Compton polarimeter installed upstream of the internal target region. The ring was filled every fifteen minutes, alternating electron helicity on successive fills.

The electrons scattered from polarized protons in a cylindrical, windowless aluminum target tube 60 cm long by 15 mm in diameter. The polarized protons were fed from an Atomic Beam Source (ABS) located above the target, well shielded against the strong, spatially varying magnetic field of the toroid [28]. A 10 mm diameter tungsten collimator in front of the target protected the cell wall coating from exposure to the beam and minimized the background rate in the detector. The ABS provided highly polarized ($P_t \sim 80\%$) isotopically pure hydrogen atoms. The spin state was randomly changed every five minutes by switching the final RF transition before the target to ensure equal target intensities for both states. The average target spin direction was oriented 48.0° to the left of the beam direction using a 0.04 T holding field.

The achieved luminosity $\mathcal{L} = 4.4 \times 10^{31}$ cm^{-2}s^{-1} of the internal gas target required the use of a large acceptance spectrometer. The symmetric detector package was built around eight copper coils which provided a maximum 0.38 T toroidal magnetic field at 6730 A, resulting in an integrated field strength of 0.15–0.44 Tm within the drift chambers for momentum analysis. Two of the eight sectors covering scattering angles of 23°–76° and ±15° out of plane were instrumented with: three drift chambers each for momentum, angle, and position determination of charged tracks, plastic scintillators for triggering and time-of-flight particle identification, and Čerenkov detectors for pion rejection. Details of the BLAST detector can be found in [29].

Data were acquired for 89.8 pb^{-1} of integrated luminosity, corresponding to 298 kC of integrated charge on the target. The elastic events were detected in coincidence with a hardware trigger requirement of scintillator signals for both the electron and proton. A second-level trigger additionally required signals in the wire chambers to reduce excessive trigger rates and to decrease the computer deadtime. The beam current was measured using a parametric direct current transformer in the ring, gated by the DAQ deadtime.

The elastic events were selected with a cut on the invariant mass of the virtual photon and the target proton system, fiducial cuts on the polar and azimuthal acceptance, and cuts on the position of the electron and proton vertex in the target cell. These cuts were consis-

tent with kinematic cuts on angle, momentum and timing correlations between the scattered electron and the recoil proton, made possible by the overdetermination of the elastic reaction. The cuts were sufficient to reduce the background to less than 1.5% without decreasing the elastic yield. The remaining background was measured with 14.9 kC of integrated charge on the same target cell without hydrogen flowing. The dependence of the background rates from the target cell wall on the target density due to a widening of the beam diameter (halo effect) was found to be negligible by comparing the quasielastic $(e,e'n)$ rates between hydrogen and empty targets.

Separate yields σ_{ij} were analyzed for each combination of electron helicity i and target spin state j, normalized by the integrated beam current. They were divided into eight Q^2 bins, listed in Table I. The event-weighted $\langle Q^2 \rangle$ was formed from the average of $\langle Q_e^2 \rangle$ (determined from the electron scattering angle) and $\langle Q_p^2 \rangle$ (from the proton recoil angle) in each bin. The yield distributions were in good agreement with results from a Monte Carlo simulation, including all detector efficiencies.

The experimental double asymmetry was formed from $(\sigma_{++} - \sigma_{+-} - \sigma_{-+} + \sigma_{--})/\Sigma\sigma_{ij}$. The beam and target single-spin asymmetries were also analyzed and served as a monitor of false asymmetries, which were found to be negligible. The experimental asymmetry was corrected for dilution by unpolarized background, including the beam halo effect. Radiative corrections were also applied using the code MASCARAD [30], but were less than 0.43% for A_r and 0.16% for A_l. The measured spin-dependent physics asymmetries are shown in Fig. 1 (upper panel), with $P_b P_t$ determined from the model-independent analysis described below, and are compared with the calculated asymmetries based on the parameterization for the proton form factors by Höhler et al. [31].

To extract the form factor ratio, the experimental asymmetries A_l and A_r were interpolated in each Q^2 bin to the average value of $\langle Q^2 \rangle$ in the left and right sectors. As discussed previously, the polarization product $P_b P_t$ and the form factor ratio $\mu_p G_E^p/G_M^p$ can be determined from the measured asymmetries A_l and A_r using Eqs. (1), (2). This way the so-called super ratio A_l/A_r would yield $\mu_p G_E^p/G_M^p$ independent of $P_b P_t$ for each Q^2 bin. In our final analysis, however, a single value of $P_b P_t$ was fit for all Q^2 values for optimal extraction of the form factor ratio [22], resulting in $P_b P_t = 0.537 \pm 0.003$ (stat) ± 0.007 (sys).

The dominant source of systematic uncertainty was the determination of $\langle Q^2 \rangle$, estimated from the difference between $\langle Q_e^2 \rangle$ and $\langle Q_p^2 \rangle$ to be less than 0.002 $(\text{GeV/c})^2$ in each bin and varying from point to point. The event-weighted average spin angle of the target with respect to the beam was $48.0° \pm 0.5°$, extracted from the analysis of the T_{20} tensor analyzing power in elastic scattering from deuterium in combination with a careful mapping of the magnetic field in the target region [32]. However, the
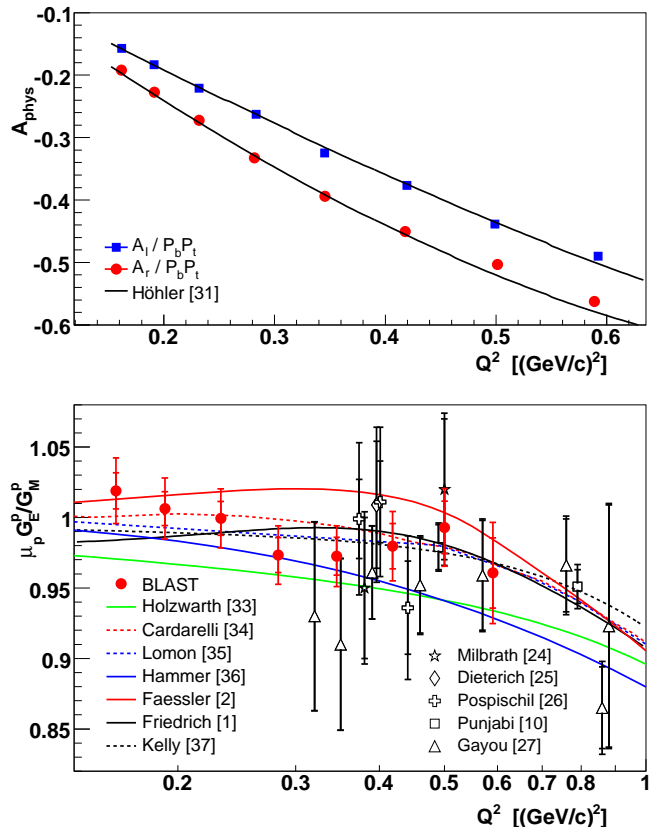

FIG. 1: Upper panel: Spin-dependent $^1\vec{\text{H}}(\vec{e}, e'p)$ asymmetry ($P_b P_t = 0.537 \pm 0.003$) compared to the expected asymmetries based on the parameterization [31] for the nucleon form factors. Lower panel: Results of $\mu_p G_E^p/G_M^p$ shown with the world polarized data [10, 24, 25, 26, 27] and several models [1, 2, 33, 34, 35, 36, 37] described in the text.

Q^2 bin	$\langle Q^2 \rangle$	A_l	A_r	$\mu_p G_E^p/G_M^p$
0.150−0.175	0.162	−0.0838(15)	−0.1022(13)	1.019±0.013±0.015
0.175−0.211	0.191	−0.0976(14)	−0.1213(14)	1.006±0.012±0.014
0.211−0.257	0.232	−0.1178(17)	−0.1453(17)	0.999±0.012±0.012
0.257−0.314	0.282	−0.1403(22)	−0.1768(20)	0.973±0.012±0.011
0.314−0.382	0.345	−0.1730(26)	−0.2100(25)	0.973±0.014±0.010
0.382−0.461	0.419	−0.2011(31)	−0.2397(33)	0.980±0.016±0.009
0.461−0.550	0.500	−0.2333(39)	−0.2686(40)	0.993±0.019±0.008
0.550−0.650	0.591	−0.2618(54)	−0.2994(57)	0.961±0.025±0.007

TABLE I: Results of measured experimental elastic asymmetries A_l, A_r (with statistical uncertainties) and extracted proton form factor ratio $\mu_p G_E^p/G_M^p \pm$ stat. $\pm$ sys. uncertainties. The values for Q^2 are given in $(\text{GeV/c})^2$.

proton form factor ratio has reduced sensitivity to the target spin angle uncertainty due to a compensation in the simultaneous extraction of $P_b P_t$.

The results are listed in Table I and are displayed in Fig. 1 with the inner error bars due to statistical uncertainties and the outer error bars being the total (statistical and systematic contributions added in quadra-

ture). Also shown in Fig. 1 are published recoil polarization data [10, 24, 25, 26, 27], together with a few selected models: a soliton model [33], a relativistic constituent quark model (CQM) with SU(6) symmetry breaking and a constituent quark form factor [34], an extended vector meson dominance model [35], an updated dispersion model [36], and a Lorentz covariant chiral quark model [2]. We also show the parameterizations by Friedrich and Walcher [1] and Kelly The impact of the BLAST results oLAST results on the separated proton charge and magnetic form factors normalized to the dipole form factor $G_D = (1 + Q^2/0.71)^{-2}$ is illustrated in Fig. 2. In this figure, Rosenbluth extractions of G_E^p and G_M^p from single experiments [12, 14, 38, 39, 40, 41, 42, 43] are presented as open triangles with statistical and total error bars, the systematic errors added in quadrature. The combined cross section data [14, 38, 39, 40, 42, 43, 44, 45, 46], obtained from [42, 47], were binned according to Table I to obtain a single L-T separation of G_E^p and G_M^p at each of the BLAST kinematics (blue circles). In comparison, the red squares show the form factors extracted from the combination of unpolarized cross sections and the measured form factor ratio from BLAST. Not only are the uncertainties reduced by a factor of 1.3–2.5, but also the negative correlation between G_E^p and G_M^p typical of L-T separations is greatly reduced. Details of the extraction will follow in a separate paper.

The proton form factors suggest a rather interesting structure around $Q^2 \approx 0.2$ to 0.5 $(\mathrm{GeV/c})^2$. While the ratio of the electric and magnetic form factors in this region is consistent with unity, the separated form factors show a deviation from the leading dependence given by the dipole form factor below 1 $(\mathrm{GeV/c})^2$. Similar structure has been observed in the neutron electric [48] and magnetic form factor [49] data as well. A possible explanation for this effect could be due to a manifestation of the pion cloud at low momentum transfer [1, 2], though a more detailed understanding of this structure is expected from chiral models and ultimately from Lattice QCD.
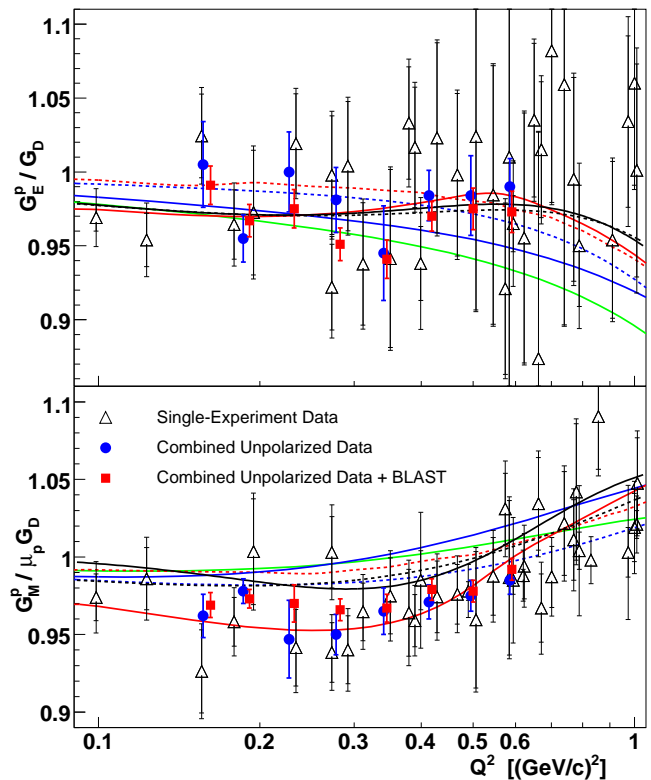
FIG. 2: Compilation of world data on G_E^p/G_D and $G_M^p/\mu_p G_D$ at BLAST kinematics with (red) and without (blue) BLAST input, shown with total uncertainties. The results from single-experiment L-T separations [12, 14, 38, 39, 40, 41, 42, 43] are shown with open symbols. The curves have the same meaning as in Fig. 1.

Rev. **D71**, 034508 (2005).

[5] D.S. Armstrong *et al.*, Phys. Rev. Lett. **95**, 092001 (2005).

[6] H. Gao, Int. J. of Mod. Phys. **E12**, 1 (2003); Erratum-ibid. **E12**, 567 (2003); C.E. Hyde-Wright and C.W. de Jager, Ann. Rev. Nucl. Part. Sci. **54**, 217 (2004).

[7] M.N. Rosenbluth, Phys. Rev. **79**, 615 (1950).

[8] T.W. Donnelly and A.S. Raskin, Ann. Phys. **169**, 247 (1986).

[9] R.G. Arnold, C.E. Carlson, and F. Gross, Phys. Rev. **C23**, 363 (1981).

[10] M. Jones *et al.*, Phys. Rev. Lett. **84**, 1398 (2000); V. Punjabi *et al.*, Phys. Rev. **C71**, 055202 (2005); Phys. Rev. **C71**, 069902(E) (2005).

[11] O. Gayou *et al.*, Phys. Rev. Lett. **88**, 092301 (2002).

[12] R.C. Walker *et al.*, Phys. Rev. **D49**, 5671 (1994).

[13] L. Andivahis *et al.*, Phys. Rev. **D50**, 5491 (1994).

[14] M.E. Christy *et al.*, Phys. Rev. **C70**, 015206 (2004).

[15] I.A. Qattan *et al.*, Phys. Rev. Lett. **94**, 142301 (2005).

[16] A. V. Belitsky, X. Ji, and Feng Yuan, Phys. Rev. Lett. **91**, 092003 (2003).

[17] J. P. Ralston and P. Jain, hep-ph/0207129; J. P. Ralston, R.V. Buniy and P. Jain, hep-ph/0206063.

[18] G.A. Miller and M.R. Frank, Phys. Rev. **C65**, 065205 (2002).

[19] S.J. Brodsky, J.R. Hiller, D.S. Hwang, V.A. Karmanov,

[1] J. Friedrich and T. Walcher, Eur. Phys. J. **A17**, 607 (2003).

[2] A. Faessler, T. Gutsche, V.E. Lyubovitskij, K. Pumsaard, Phys. Rev. **D73**, 114021 (2006).

[3] M.R. Schindler, J. Gegelia, and S. Scherer, Eur. Phys. J. **A26**, 1 (2005).

[4] H.H. Matevosyan, G.A. Miller, and A.W. Thomas, Phys. Rev. **C71**, 055204 (2005); R.G. Edwards, Nucl. Phys. Proc. Suppl. **140**, 290 (2005); M. Göckeler *et al.*, Phys.

Phys. Rev. **D69**, 076001 (2004).

[20] P.A.M. Guichon and M. Vanderhaeghen, Phys. Rev. Lett. **91**, 142303 (2003); P.G. Blunden, W. Melnitchouk, and J.A. Tjon, Phys. Rev. Lett. **91**, 142304 (2003); M.P. Rekalo and E. Tomasi-Gustafsson, Eur. Phys. J. **A22**, 331 (2004).

[21] Y.C. Chen, A. Afanasev, S.J. Brodsky, C.E. Carlson and M. Vanderhaeghen, Phys. Rev. Lett. **93**, 122301 (2004); A.V. Afanasev and N.P. Merenkov, Phys. Rev. D **70**, 073002 (2004).

[22] C.B. Crawford, Ph.D. thesis, Massachusetts Institute of Technology (2005).

[23] A.T. Sindile, Ph.D. thesis, University of New Hampshire (2006).

[24] B. Milbrath *et al.*, Phys. Rev. Lett. **80**, 452 (1998); Phys. Rev. Lett. **82**, 2221(E) (1999).

[25] S. Dieterich *et al.*, Phys. Lett. **B500**, 47 (2001).

[26] T. Pospischil *et al.*, Eur. Phys. J. **A12**, 125 (2001).

[27] O. Gayou *et al.*, Phys. Rev. **C64**, 038202 (2001).

[28] D. Cheever *et al.*, Nucl. Instr. Meth. **A556**, 410 (2006); L.D. van Buuren *et al.*, Nucl. Instr. Meth. **A474**, 209 (2001).

[29] D. Hasell *et al.*, The BLAST Experiment, to be published.

[30] A. Afanasev, I. Akushevich, and N. Merenkov, Phys. Rev. **D64**, 113009 (2001).

[31] G. Höhler *et al.*, Nucl. Phys. **B114**, 505 (1976).

[32] C. Zhang *et al.*, to be published.

[33] G. Holzwarth, Z. Phys. **A356**, 339 (1996).

[34] F. Cardarelli and S. Simula, Phys. Rev. **C62**, 065201 (2000); S. Simula, e-print nucl-th/0105024.

[35] E.L. Lomon, Phys. Rev. **C66**, 045501 (2002).

[36] H.-W. Hammer and Ulf-G. Meissner, Eur. Phys. J. **A20**, 469 (2004).

[37] J.J. Kelly, Phys. Rev. **C70**, 068202 (2004).

[38] T. Janssens *et al.*, Phys. Rev. **142**, 922 (1966).

[39] M. Goitein *et al.*, Phys. Rev. **D1**, 2449 (1970); L.E. Price *et al.*, Phys. Rev. **D4**, 45 (1971).

[40] C. Berger *et al.*, Phys. Lett. **B35**, 87 (1971).

[41] W. Bartel *et al.*, Nucl. Phys. **B58**, 429 (1973).

[42] F. Borkowski *et al.*, Nucl. Phys. **A222**, 269 (1974); Nucl. Phys. **B93**, 461 (1975);

[43] P.E. Bosted *et al.*, Phys. Rev. **C42**, 38 (1990).

[44] W. Bartel *et al.*, Phys. Rev. Lett. **17**, 608 (1966);

[45] S. Stein *et al.*, Phys. Rev. **D12**, 1884 (1975).

[46] M.I. Niculescu, Ph.D. thesis, Hampton University (1999).

[47] J. Arrington, Phys. Rev. **C69**, 022201(R) (2004).

[48] D.I. Glazier *et al.*, Eur. Phys. J. **A24**, 101 (2005); B. Plaster *et al.*, Phys. Rev. **C73**, 025205 (2006).

[49] W. Xu *et al.*, Phys. Rev. Lett. **85**, 2900 (2000); W. Xu *et al.*, Phys. Rev. **C67**, 012201(R) (2003).